Integration of renewable source with non -ideal grid conditions using new converter control

Siva Sai Praveen K[1], V Rammohan G[2]

[1]Student, Department of EEE, Kakinada Institute of Science and Technology, Kakinada, Andhra Pradesh, India.

[2]Assistant Professor, Department of EEE, Kakinada Institute of Science and Technology, Kakinada, Andhra Pradesh, India.

Corresponding Author: kssaipraveen746@gmail.com

Abstract: - This paper presents the distributed sparce based voltage source converter (VSC) control for three-phase grid tied inverters interfacing distributed renewable resources (DERs) into the power grid. An uncertainty and disturbance modelling based control law is developed for achieving the robustness against nonideal grid conditions including the grid impedance variations, grid voltage harmonics and fluctuations in grid voltage magnitude (symmetrical/ asymmetrical), frequency and phase. The distributed sparce control performs multitasks. It feeds the generated solar PV power to the local three phase grid. It reduces the harmonics of loads and furnished a balanced current of local three-phase grid. The distributed sparce control uses a solar PV array, a voltage source converter, a nonlinear load, a three-phase grid, DC-link capacitance. By Using this distributed sparce control, extract maximum power condition from PV system with single stage converter, so number of power electronic components reduced. For extracting maximum power from the PV source, the traditional P&O (Perturb and Observe) scheme is utilized here. The tracking performance and efficiency of P&O technique, are also examined here at rapid changing climatic conditions to show behavior of P&O scheme. The distributed sparce control approach is capable to estimate required fundamental component to find out reference grid currents.

Key Words— Perturb and Observe scheme, Distributed renewable resources

I. INTRODUCTION

GRID-TIED inverters (GTIs) play an important role in integrating different types of distributed energy resources (DERs) into the distribution networks or micro-grids for controlling the current injection, while simultaneously improving the power quality [1-3]. However, since the distribution networks or micro-grid for DERs integration are typically electrically weak and traditionally suffer from poor voltage quality at the end buses or unstable point of common coupling (PCC) voltage when the micro-grid operated in an islanded mode, any non-ideal grid conditions (e.g., harmonics, magnitude/ frequency/ phase variation) caused by external disturbances may adversely affect the grid injected current quality and the stability of inverter control [4], [5]. Moreover, depending on the grid configuration, the grid impedance, which is mainly determined by low power transformers and long distributed lines, varies over a wide range, especially in the weak grids [6-7].

It should be noted that when the micro-grid for the GTI integration changes the operation mode (i.e., from grid-connected mode to islanded mode), the PCC voltage is maintained via other grid-forming units, while the grid impedance will be affected significantly [8]. It is a considerable challenge for GTIs to continue their stable operation and to supply high-quality sinusoidal current from DERs with a smoother transient response under such conditions. In an ideal grid condition, typical control strategy such as PI or PR control is commonly used for current-controlled inverters. Since its implementation and design are rather simple and well known from the L filter control [9], it is sufficient to ensure good performance in both steady-state and transient-state via the internal current control loop [10-12]. However, when dealing with the LCL filter and the grid impedance becomes relatively high, which may result in a less damped system, the poles are attracted to the imaginary axis, then the stability margin is degraded and the low-frequency gain and bandwidth will be limited, consequently the tracking performance and disturbance rejection capability of the current controller can be decreased [13].

II. CONTROL TECHNIQUE

A. MPPT Algorithm:

There are various MPPT methods reported in [8]. The P&O scheme is used in this work for harnessing maximum power from SPEGS [9]. The MPPT initially needs to take two points of solar panel voltage and solar array current and generates reference DC link voltage Vdc*.

B. Distributed Sparse Based VSC Control:

Fig. 1 provides the block of distributed sparse control for proposed system. Following variables are sensed for implementation of proposed control approach, which are PV voltage and current (V_{PV}, I_{PV}), grid currents (i_{ga}, i_{gb}), load current (i_{La}, i_{Lb}) and a point of interconnection voltages (v_{ga}, v_{gb}). The amplitude of PCI voltage is obtained as,

International Journal of Progressive Research in Science and Engineering
Volume-1, Issue-5, August-2020
www.ijprse.com

$$V_t = \sqrt{\frac{2}{3}\left(v_{ga}^2 + v_{gb}^2 + v_{gc}^2\right)} \tag{1}$$

Where, the voltages of all three phases, are calculated from the recorded line voltages as,

$$v_{ga} = \frac{2v_{gab} + v_{gbc}}{3}; v_{gb} = \frac{-v_{gab} + v_{gbc}}{3}; v_{gc} = \frac{-v_{gab} - v_{gbc}}{3} \tag{2}$$

With the help of phase voltages, the in-phase unit templets are calculated as,

$$u_{pam} = \frac{v_{ga}}{V_t}; u_{pbm} = \frac{v_{gb}}{V_t}; u_{pcm} = \frac{v_{gc}}{V_t} \tag{3}$$

C. Implementation of Distributed Sparse Control:

As it is given in [20, 21], utilizing distributed estimation method gives spatial diversity. Due to this, the performance in comparison with a local adaptive filter, is improved. Therefore, for integrating a SPEGS into the grid, a novel distributive sparse based control technique is proposed in this section. The effectiveness of any distributed scheme is significantly influenced by co-operation that are allowed among the nodes [21]. In this case, a network is considered with m node adaptive technique. Here, the objective of every one, is to calculate the unspecified sparse vector D_{wpa0}. In this scheme, as depicted in Fig.3, every node m, cooperates with its neighbor-hood nodes, Pm which is explained as a combination of nodes connected to node m with inclusion of node m also. By this approach, node m connects to its local estimate, $D_{Wpam(n)}$ with its nebiour hood estimations, {$D_{Wlm(n)}$, l belongs to Pm}, which is estimated as [21],

$$\lambda_{pam}(n) = \sum_{l \in p_m} \sigma_{lm} D_{Wlm} \tag{4}$$

Here, σlm represents the weight of co-operation, which is selected as in [19, 20]. By combining the observed estimate at the neighborhood of m, the estimated $D_{wpam(n)}$ replaced by λ_{pam} (n), as calculated in (4) for some co-operation coefficient (**σ**lm≥0). This calculated estimation (4) at node m, gives an adaptive estimation with co-operation factor of Dwlm0 given the {D_{wlmn}} at every neighbor node of m. The co-operation step combined information from nodes over the network into node m. This happens, because each node in Pm tends to have various neighbor-hood, as shown in Fig. 2. The error signal is obtained as [20, 21],

$$e_{pam}(n) = i_{La}(n) - \lambda_{pam}(n)^T u_{pam}(n) \tag{5}$$

Here em(n) denotes the error, which is reduced in every step by proper updating of the fundamental component of weight for load current. In (4.4), the calculated estimation with cooperation factor, λ_{pam} at node m can feed into the local information and find final estimation D_{wpam}. Now, based on

above error signal and calculated estimation with cooperation factor λ_{pam} at node m, the fundamental component of load current of phase 'a' is estimated as [19],
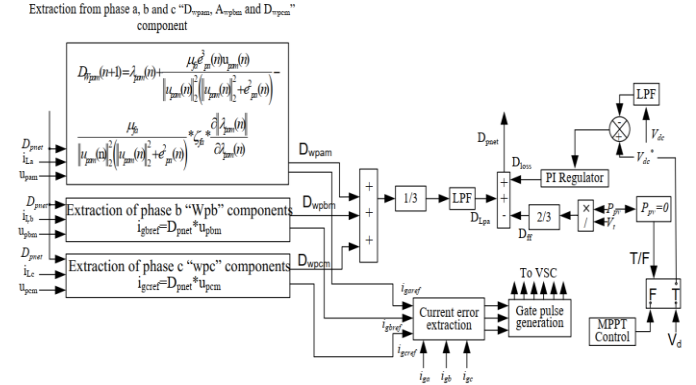

Fig.1. Block diagram for proposed control

$$D_{wpam}(n+1) = \lambda_{pam}(n) + \frac{\mu_{fa} e_{pa}^3(n)\mu_{pam}(n)}{\Box \mu_{pam}(n)\Box_2^2 \left(\Box \mu_{pam}(n)\Box_2^2 + e_{pa}^2(n)\right)} - \tag{6}$$

$$\frac{\mu_{fa}}{\Box \mu_{pam}(n)\Box_2^2\left(\Box \mu_{pam}(n)\Box_2^2 + e_{pa}^2(n)\right)} * \zeta_{fa} * \frac{\partial \Box \lambda_{pam}(n)\Box}{\partial \lambda_{pam}(n)}$$

Similarly, for phase 'b' and phase 'c', the fundamental weight components of load currents are estimated as,

$$D_{wpam}(n+1) = \lambda_{pbm}(n) + \frac{\mu_{fa} e_{pb}^3(n)\mu_{pbm}(n)}{\Box \mu_{pbm}(n)\Box_2^2 \left(\Box \mu_{pbm}(n)\Box_2^2 + e_{pb}^2(n)\right)} - \tag{7}$$

$$\frac{\mu_{fa}}{\Box \mu_{pbm}(n)\Box_2^2\left(\Box \mu_{pbm}(n)\Box_2^2 + e_{pb}^2(n)\right)} * \zeta_{fb} * \frac{\partial \Box \lambda_{pbm}(n)\Box}{\partial \lambda_{pbm}(n)}$$

$$D_{wpcm}(n+1) = \lambda_{pcm}(n) + \frac{\mu_{fc} e_{pc}^3(n)\mu_{pcm}(n)}{\Box \mu_{pcm}(n)\Box_2^2 \left(\Box \mu_{pcm}(n)\Box_2^2 + e_{pc}^2(n)\right)} - \tag{8}$$

$$\frac{\mu_{fc}}{\Box \mu_{pcm}(n)\Box_2^2\left(\Box \mu_{pcm}(n)\Box_2^2 + e_{pc}^2(n)\right)} * \zeta_{fa} * \frac{\partial \Box \lambda_{pcm}(n)\Box}{\partial \lambda_{pcm}(n)}$$

D. Switching Pulses for VSC:

By equating the sensed DC link voltage (Vdc) and estimated DC link voltage (Vdc*), the loss factor is obtained, which is given to the PI (Proportional-Integral) controller to control the DC link voltage to the defined value. The error is obtained as

$$V_{dc\_error}(n) = V_{dc}^*(n) - V_{dc}(n) \tag{9}$$

Here, if solar power becomes unavailable (i.e. PPV=0), Vdc* moves to reference DC link voltage. The PI regulator output is obtained as,

$$D_{loss}(n+1) = D_{loss}(n) + K_p\left\{V_{dcerror}(n+1) - V_{dcerror}(n)\right\} + K_I V_{dcerror}(n+1) \tag{10}$$

Here, distributed weight of active loss is represented by Dloss. At the moment, when VSC is switching, active power drawn by distribution feeder is selected as adaptive loss term Dloss,

which is utilized for maintaining the self-healing of DC-link voltage to minimize the steady state fluctuation in DC-link voltage. To enhance the dynamic performance of the PV system under varying climatic condition, a feed-forward term is estimated as,

$$D_{ff} = \frac{2P_{pv}}{3V_t} \qquad (11)$$

Here, Vt is amplitude of PCI voltage estimated in (4.1). The active power component of utility grid (DPnet) is estimated as,

$$D_{pnet} = D_{Lpa} + D_{loss} - D_{ff} \qquad (12)$$

Here, DLpa denotes the equivalent average load component of all three phase, which is calculated to perform load balancing and expressed as,

$$D_{Lpa} = \frac{(D_{wpam} + D_{wpbm} + D_{wpcm})}{3} \qquad (13)$$

Moreover, the reference currents for local distribution
Moreover, the reference currents for local distribution

$$i_{garef} = D_{Lpa} * u_{pam}; i_{gbref} = D_{Lpb} * u_{pbm}; i_{gcref} = D_{Lpc} * u_{pcm} \qquad (14)$$

An indirect current control approach with hysteresis controllers, is used to getting the switching pulses for VSC. Therefore, the current errors for hysteresis controller are calculated as,

$$i_{ga\_error} = i_{ga} - i_{garef}; i_{gb\_error} = i_{gb} - i_{gbref}; i_{gc\_error} = i_{gc} - i_{gcref} \qquad (15)$$

III. PROPOSED SYSTEM

A multi-mode single stage SPEGS is depicted in Fig. 2. It comprises of a single converter, which is a voltage source converter (VSC) for harnessing optimum power via MPPT as well as to feed the solar power from source to the three phase weak distribution network and to assist it via facilitating some additional features like harmonics minimization, grid currents balancing and power factor improvement as a DSTATCOM without any additional device. Interfacing inductors are used between VSC and the distribution network to minimize the switching losses and subsequently, smoothens the distribution network currents.
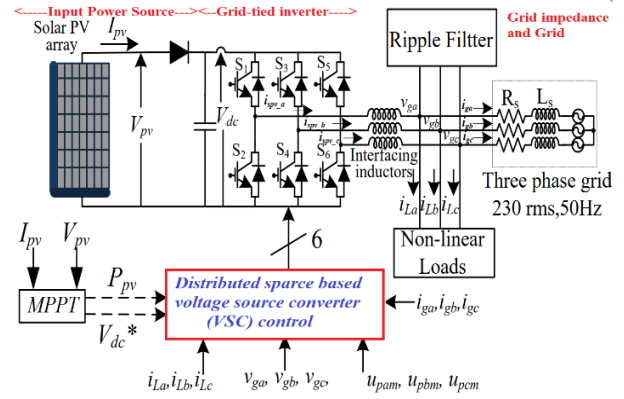

Fig.2. Block diagram of SPV-grid System

A high pass ripple filter is utilized at PCI (Point of Common Interconnection) to absorb the switching ripple produced at VSC. Detailed design and rating selection of different components, which are used in the proposed system, are made based on the procedure given in [14, 23]. Fig. 2 shows the proposed control of SPEG system interfaced to the three-phase distribution network. This control consists of MPPT scheme and VSC switching. The MPPT scheme is achieved by P&O based scheme as well as the VSC control methodology is executed via adaptive based approach.

IV. RESULTS AND DISCUSSION

In this section, the proposed robust control method is tested and compared with the PI controller-based grid-side current feedback control strategy [15] and the distributed sparce control strategy [16] through Matlab/Simulink simulations. In the simulation tests, two cases are considered to testify the performance of the proposed controller.

A. Harmonic rejection capability

In this case, the system is operated in an MPPT mode with SW1 off. The programmable AC source is used to simulate the grid voltage distorted by 5th, 8th, 11th, 13th and 23rd harmonics. The magnitude of harmonics with respect to the fundamental grid voltage is 5%, 3%, 2%, 2% and 1%, respectively, and the corresponding phases are 180°, 0°, 0°, 0° and 0°. In the meantime, the solar irradiance is varied from 1000 W/m2 to 800W/m2 at t =1 s, then increased to 1200 W/m2 at t =1.2 s. For the proposed controller, the maximum active power point can be obtained by the MPPT operation in the case of solar irradiance variation, as shown in Fig. 3. (a).

International Journal of Progressive Research in Science and Engineering
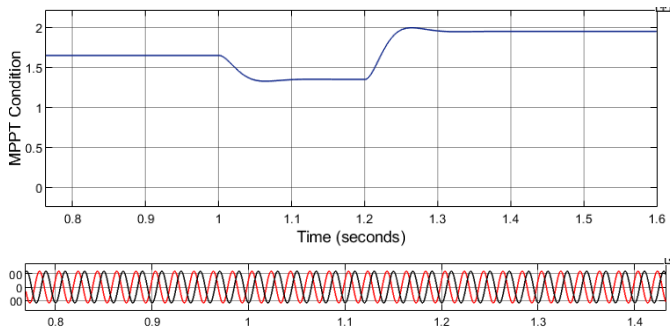Volume-1, Issue-5, August-2020
www.ijprse.com

Fig.3. Performance of the proposed controller under a distorted grid voltage when the system operated in an MPPT mode. (a) MPPT command and grid current (b) Current tracking performance in stationary frame and the tracking errors.

Also, it can be seen that the grid feeding current is pure sinusoidal with high harmonic rejection ability, and can properly follow the changed power command with almost invisible oscillation. Furthermore, it can be observed in Fig. 3.(b) that the α - and β -axis current components can faithfully track the desired trajectories with minimal tracking errors (less than 0.2A).

B. Asymmetrical fault rides through

The asymmetrical fault is emulated by the programmable ac source and firstly occurs at 0.3s with $v_{ga} = 0.8\angle 0\,°$, $v_{gb} = 0.5\ \angle -120\,°$ and $v_{gc} = 1\ \angle 120\,°$ in p.u., and lasts for about 0.3s before it returns to normal, then another fault happens at 0.98s with 30% voltage drop as well as phase shift and frequency variation from 50Hz to 51Hz as shown in Fig. 5.2 (a).
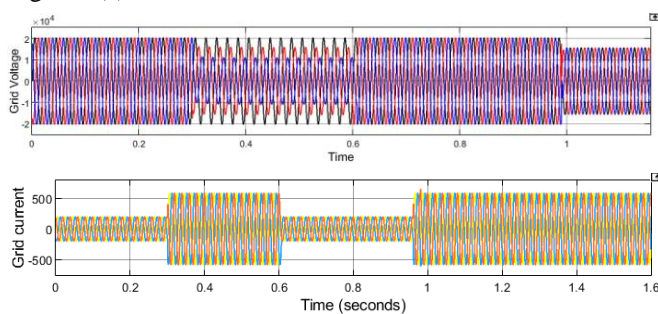

Fig. 4. Performance of the controllers under asymmetrical grid voltage and frequency variation. (a) Faulty grid voltage. (b) Grid current of the proposed controller.

Comparison between the proposed controller and the PR controller are investigated with the same current references in a stationary frame. It can be seen from Fig.4 (a) and Fig. 4 (b) that both of them maintain sinusoidal and three-phase balanced grid current, despite the unbalanced fault of the grid voltage is serious.

V. CONCLUSION

This project presents the design of a distributed sparce based voltage source converter (VSC) control to integrate the SPVs to the grid while achieving robust current control under varying grid impedances and various grid voltage disturbances, such as harmonic pollution, magnitude (symmetrical/ asymmetrical) variations, and frequency, phase shift. Strong robustness and superior current tracking performance can be simultaneously ensured for external disturbance rejection and high-quality current injection. The smooth transient response can be ensured since the dynamic of the controller is fast. The stability of the proposed control is analyzed, and the effectiveness of the proposed control strategy is verified through simulation studies. Dynamic behavior of proposed control technique, has been observed better in comparison with existing control approaches. The proposed approach has worked well in all scenarios at unity power factor operation and resolves problems related to power quality of grid. The THD of grid currents, is obtained in the limit of the IEEE-519 standard [22].

REFERENCES

[1] A. M. Bouzid, J. M. Guerrero, A. Cheriti, M. Bouhamida, P. Sicard, and M. Benghanem, "A survey on control of electric power distributed.

[2] F.A. Farret and M.G. Simões, Integration of Alternative Sources of Energy, John Wiley & Sons, Inc., 2006.

[3] L Robert Foster, Majid Ghassemi and Alma Cota, "Solar Energy Renewable Energy and the Environment," CRC Press FL 2010.

[4] Mu Zhou, "Report for reviewing the renewable energy and energy saving in USA", Journal of Renewable Energy, vol. 25, no.1, PP. 98-101, 2007.

[5] S. Reichelstein and M. Yorston, "The prospects for cost competitive solar PV power special section: Long run transitions to sustainable economic.

[6] F. Locment, M. Sechilariu and I. Houssamo, "DC Load and Batteries Control Limitations for Photovoltaic Systems. Experimental Validation," IEEE Trans. Power Electronics, vol.27, no.9, pp.4030,4038, Sept. 2012.

[7] Caisheng Wang and M. H. Nehrir, "Power Management of a Stand-Alone Wind/Photovoltaic/Fuel Cell Energy System," IEEE Transactions on Energy Conversion, vol.23, no.3, pp.957-967, Sept. 2008.

[8] S. Jain and V. Agarwal, "Comparison of the performance of maximum power point tracking schemes applied to single-stage grid-connected photovoltaic systems," IET Electric Power Applications, vol. 1, no. 5, pp. 753-762, Sept. 2007.

[9] B. Subudhi and R. Pradhan, "A Comparative Study on Maximum Power Point Tracking Techniques for Photovoltaic Power Systems," IEEE Transactions on Sustainable Energy, vol. 4, no. 1, pp. 89-98, Jan. 2013.

[10] R. K. Agarwal, I. Hussain and B. Singh, "LMF-Based Control Algorithm for Single Stage Three-Phase Grid Integrated Solar PV System," IEEE Trans. Sustainable Energy, vol. 7, no. 4, pp. 1379-1387, Oct. 2016.

[11] S.B. Kjaer, J.K. Pedersen, F. Blaabjerg, "A review of single-phase grid connected inverters for photovoltaic modules," IEEE Transactions on Industry Applications, vol.41, no.5, pp.1292-1306, Sept.-Oct. 2005.

[12] F. Chan and H. Calleja, "Reliability Estimation of Three Single-Phase Topologies in Grid-Connected PV Systems," IEEE Transactions on Industrial Electronics, vol.58, no.7, pp.2683-2689, July 2011.

[13] Antonio Moreno Munoz, Power Quality: Mitigation Technologies in a Distributed Environment, Springer-Verlag, London, 2007.

[14] Ambra Sannino, Jan Svensson and Tomas Larsson, "Review power electronic solutions to power quality problems, "Journal of Electric Power Systems Research, vol. 66, pp.71-82, 2003.

[15] B. Singh, A. Chandra, and K. Al-Haddad, Power Quality: Problems and Mitigation Techniques. Chichester, U.K.: Wiley, 2015.

[16] B. Singh, S. K. Dube, S. R. Arya, A. Chandra and K. Al-Haddad, "A comparative study of adaptive control algorithms in Distribution Static Compensator," in Proc. of IEEE Annual Conference of Industrial Electronics Society (IECON), 2013, pp.145-150.

[17] Parmod Kumar and A. Mahajan, "Soft Computing Techniques for the Control of an Active Power Filter," IEEE Transactions on Power Delivery, vol.24, no.1, pp.452-461, Jan. 2009.

[18] Chao-Shun Chen, Chia-Hung Lin, Wei-Lin Hsieh, Cheng-Ting Hsu and Te-Tien Ku, "Enhancement of PV Penetration with DSTATCOM in Taipower Distribution System," IEEE Transactions on Power Systems, vol.28, no.2, pp.1560-1567, May 2013.

[19] B. Singh, D. T. Shahani and A. K. Verma, "Neural Network Controlled Grid Interfaced Solar Photovoltaic Power Generation," IET Power Electronics, vol.7, no.3, pp. 614-626, July 2013.

[20] A. H. Sayed and C. G. Lopes, "Distributed processing over adaptive networks," 9th International Symposium on Signal Processing and Its Applications, Sharjah, 2007, pp. 1-3.

[21] M. Hajiabadi and H. Zamiri-Jafarian, "Distributed adaptive LMF algorithm for sparse parameter estimation in Gaussian mixture noise," 7'th Inter. Symp. Telecommun. (IST'2014), Tehran, 2014, pp. 1046-1049.

[22] IEEE Recommended Practices and requirement for Harmonic Control on Electric Power System, IEEE Std.519, 1992.

[23] M. Villalva, J. Gazoli and E. Filho, "Comprehensive approach to modeling and simulation of photovoltaic arrays," IEEE Trans. Pow. Elec., vol.24, no.5, pp.1198-1208, May 2009.